Biogeosciences Discuss., 8, 1985–2013, 2011
www.biogeosciences-discuss.net/8/1985/2011/
doi:10.5194/bgd-8-1985-2011

Biogeosciences Discussions

Application of δ^{13}C and δ^{15}N isotopic signatures of organic matter fractions sequentially separated from adjacent arable and forest soils to identify carbon stabilization mechanisms

Z. E. Kayler[1], M. Kaiser[2], A. Gessler[1], R. H. Ellerbrock[3], and M. Sommer[3]

[1]Institute for Landscape Biogeochemistry, Leibniz-Center for Agricultural Landscape Research (ZALF), Eberswalderstr. 84, 15374 Müncheberg, Germany
[2]University of California – Merced, 4225 N. Hospital Road, Atwater 95301, California, USA
[3]Institute of Soil Landscape Research, Leibniz-Center for Agricultural Landscape Research (ZALF), Eberswalderstr. 84, 15374 Müncheberg, Germany

Received: 28 January 2011 – Accepted: 14 February 2011 – Published: 1 March 2011

Correspondence to: Z. E. Kayler (zachary.kayler@zalf.de)

Published by Copernicus Publications on behalf of the European Geosciences Union.

Abstract

Identifying the chemical mechanisms behind soil carbon bound in organo-mineral complexes is necessary to determine the degree to which soil organic carbon is stabilized belowground. We used the δ^{13}C and δ^{15}N isotopic signatures from two organic matter (OM) fractions from soil to identify the likely binding mechanisms involved. We used OM fractions hypothesized to contain carbon stabilized through organo-mineral complexes: (1) OM separated chemically with sodium pyrophosphate (OM(PY)) and (2) OM stabilized in microstructures found in the chemical extraction residue (OM(ER)). Furthermore, because the OM fractions were separated from five different soils with paired forest and arable land use histories, we could address the impact of land use change on carbon binding and processing mechanisms within these soils. We used partial least squares regression to analyze patterns in the isotopic signature of OM with established proxies of different binding mechanisms. Parsing soil OM into different fractions is a systematic method of dissection, however, we are primarily interested in how OM is bound in soil as a whole, requiring a means of re-assembly. Thus, we implemented the recent zonal framework described by Kleber et al. (2007) to relate our findings to undisturbed soil.

The δ^{15}N signature of OM fractions served as a reliable indicator for microbial processed carbon in both arable and forest land use types. The δ^{13}C signature of OM fractions in arable sites did not correlate well with proxies of soil mineral properties while a consistent pattern of enrichment was seen in the δ^{13}C of OM fractions in the forest sites. We found a significant difference in δ^{13}C of pooled OM fractions between the forest and arable land use type although it was relatively small (<1‰). We found different binding mechanisms predominate in each land use type. The isotopic signatures of OM fractions from arable soils were highly related to the clay and silt size particles amount while organic matter not directly bound to mineral surfaces in the contact zone was involved in cation bonding with Ca. In forest soils, we found a relationship between isotopic signatures of OM(PY) and the ratio of soil organic carbon content to

soil surface area (SOC/SSA). For arable soils, the formation of OM(PY)-Ca-mineral associations seems to be a relevant OM stabilization mechanism while the OM(PY) of forest soils seems to be separated from layers of slower exchange not directly attached to mineral surfaces. This means there is a potential to build multiple OM layers on mineral particles in the arable soil and thus the potential for carbon accumulation.

1 Introduction

Forest and agricultural soils are potential carbon sinks that can help mitigate the current trajectories of climate change effects on the terrestrial biosphere. Carbon storage belowground is balanced by carbon losses and inputs, hence, soil carbon stocks will accumulate by increasing the mean residence time of carbon sent belowground (Smith et al., 1997; Lal, 2004). Organic matter (OM) is a complex mixture of organic compounds at different stages of decomposition posing a significant problem of characterizing the residence time of carbon belowground based on an understanding of chemical and physical properties (Kleber and Johnson, 2010). Ongoing challenges facing soil scientist and biogeochemists are to define and quantify which organic molecules are stabilized, how long carbon molecules persist in soil, and to identify the underlying stabilization and destabiliation mechanisms.

Currently, OM is considered stabilized in soil when it is protected from microbial oxidation by (i) occlusion in aggregates (Bachmann et al., 2008), (ii) interactions with polyvalent cations (OM-cation complexes), (iii) via polyvalent cations with soil mineral surfaces (OM-mineral associations) (von Lützow et al., 2006) or OM is preserved due to freezing temperatures, low O_2 content or water saturation (climatic stabilization; Trumbore, 2009). To characterize OM binding mechanisms in soil, soil OM is generally divided into operationally defined fractions that are hypothesized to contain carbon stabilized by the mechanisms previously described (Mikutta et al., 2006; von Lützow et al., 2007; Sollins et al., 2009). Specifically, an extraction with Na-pyrophosphate

solution separates soil OM that interacts with polyvalent cations (forming OM-cation complexes) (Masiello et al., 2004) and OM that interacts via polyvalent cations with soil mineral surfaces (forming OM-mineral associations) (Wattel-Koekkoek et al., 2003; Kögel-Knabner et al., 2008). Consequently, Na-pyrophosphate soluble fractions are primarily comprised of OM stabilized through complexes formed with soil mineral compounds (Kaiser et al., 2011).

Experiments using changes in C3/C4 vegetation, have interpreted the stable isotopic signature (δ^{13}C and δ^{15}N) of soil fractions to determine mean residence times (Liao et al., 2006; Haile-Mariam et al., 2008; Ellerbrock and Kaiser, 2005), the impact of vegetation change (Solomon et al., 2002), impact of mining disturbance (Wick et al., 2009), and isotope fractionation determined by Rayleigh distillation (Clay et al., 2007). However, the potential to use the isotopic signature of soil OM fractions to reveal OM binding mechanisms that lead to stabilization has not been fully realized. Studies that have analyzed the isotopic signature of soil OM fractions (beyond C3/C4 labeling techniques) have found patterns of enrichment of δ^{13}C and δ^{15}N with increasing density of sequentially separated OM fractions (Huygens et al., 2008; Sollins et al., 2009; Marin-Spiotta et al., 2010). They attributed these patterns to isotope discrimination during microbial processing whereby microbes consume OM, respire the light isotope (carbon) and incorporate the heavy isotope (carbon and nitrogen) into biomass that is subsequently deposited in the soil OM complex. Indeed, Huygens et al. (2008) found a high degree of microbial biomarkers in soil microaggregates, providing strong evidence that microbial processing of OM is an important step towards organic matter stabilization.

Analysis of δ^{13}C and δ^{15}N isotopic signatures of stabilized OM fractions along with soil mineral characteristics may yield important information about OM-mineral associations and their processing history. For example, oxalate extractable Al and Fe contents are established proxies for poorly crystalline minerals, which form stable complexes with OM via ligand exchange reactions (Kleber et al., 2005; Mikutta et al., 2006), while polyvalent cations such as Ca^{2+} and Fe^{3+} play an important role in bridging OM to

mineral surfaces (Oades, 1988; Baldock and Nelson, 2000; Wuddivira and Camps-Roach, 2006). Thus, analyses of these proxies along side with patterns in stable isotopes can be used to characterize the OM fractions as microbially processed or not and potentially identify which binding mechanisms predominate.

Breaking down soil OM into different fractions is necessary to identify which OM is stabilized, but we need a method of re-assembly to understand how OM and the different binding mechanisms are arranged in the organo-mineral complex. Kleber et al. (2007), provided such a tool by incorporating different binding mechanisms into a zonal, structural model specific to organo-mineral interactions. While a detailed discussion of the model is beyond the scope of this paper, the model does provide a framework to interpret the exchange and isotopic signatures of OM directly interacted with mineral surfaces or present in subsequently attached layers. The model describes a zone of direct interaction between OM and mineral surfaces (contact zone), a zone dominated by hydrophobic interactions and a kinetic zone of OM crosslinked via polyvalent cations. Each zone represents different levels of stabilization, the strongest being the contact zone while weak interactions between mineral surfaces and OM occur in the kinetic zone.

We analyzed the isotopic signal of OM fractions sequentially separated from a range of soil types under arable and forest land use to investigate patterns of microbial transformations in different OM fractions and to determine the type of interaction between OM and soil minerals. We focused on the $\delta^{13}C$ and $\delta^{15}N$ of (i) OM sequentially extracted by a Na-pyrophosphate solution (OM(PY)) after separating organic particles and water-extractable OM (Kaiser et al., 2011) and (ii) OM remaining in the extraction residue (OM(ER)); both fractions are hypothesized to contain stabilized carbon. We compared common soil mineral parameters (i.e., specific surface area, contents of clay, oxalate soluble, and exchangable cations) with isotopic data using a partial least squares regression analyses (PLS), which enabled us to draw conclusions about mechanisms behind OM stabilization. We then used the zonal model, which provides molecular resolution to OM stabilization, and the molecular characterization of the OM

present in the fractions as determined by stable isotopes, to characterize the structure of the organo-mineral interaction for each land use type.

2 Methods

2.1 Site selection and soil sampling

We selected 5 sites within Germany (Table 1) characterized by different soil types and mineral properties (Table 2). Two land use types, arable and forest, were present in close proximity at each site. The land uses have bee in practice for at least 100 yr. The selected soils were classified according to World Reference Base for Soil Resources (2006) as Albic Luvisol (AL), Haplic Stagnosol (HSt), Haplic Cambisol (HC), Haplic Luvisol (HL), and Vertic Cambisol (VC). Kaiser et al. (2009), provides further details on soil sampling description.

2.2 Physicochemical characterization of soil samples

The pH values, and SOC, clay, silt, and sand contents were analysed as given in Kaiser et al. (2009). The amount of exchangeable cations (Ca_{ex}) were determined from 5 g soil according to Deutsche Industrie Norm (DIN) 19684 (1977) using Inductive Coupled Plasma Optical Emission Spectroscopy (ICP-OES; Type 138, Jobin Yvon Ltd, München, Germany) (DIN EN ISO 11885 (1998)) and corrected by using data from blank solutions. The oxalate soluble Al and Fe (Fe_{ox}, Al_{ox}) were extracted according to Schlichting et al. (1995), and the contents of Al and Fe in solution were determined using ICP-OES (DIN EN ISO 11885 (1998)). All analyses were done in duplicates and the data were normalized to 105 °C dry soil. To assess the specific surface area (SSA) of the soil mineral phase, the OM was oxidized (Kaiser and Guggenberger, 2003) using a NaOCl solution (6%, adjusted to pH 8.0 with concentrated HCl) at a soil-to-solution ratio of 1:10 at 25 °C for 6 h (Siregar et al., 2004). The samples were centrifuged, and

the supernatants were removed. The NaOCl-treatment was repeated five times (Kaiser and Guggenberger, 2003). The remaining solid residues were then washed once with de-ionised water and centrifuged. The supernatant was removed, and the solid residue was shaken with de-ionised water overnight. After that, the NaOCl treated topsoil samples were dialysed and then freeze-dried (Siregar et al., 2004). The SSA of the freeze dried solid residue was determined by N_2 adsorption (Quantasorb, QUANTACHROME CORP., Syosset, NY, USA). The NaOCl treatment did not remove the OM completely from the soil so we corrected the SSA values as determined after the NaOCl treatment according to Mikutta et al. (2005). The corrected SSA values are given in Table 2.

2.3 Sequential separation of Na-pyrophosphate ($Na_4P_2O_7$) soluble OM (OM(PY)) and OM remaining in extraction residue OM(ER)

1. Following the methods of Kaiser et al. (2009, 2010) we sequentially separated the physically uncomplexed, macro- and micro-aggregate occluded organic particle and water-extractable OM from air-dried (< 2 mm) soil sample by a combination of electrostatic attraction, ultra-sonication (60 and 440 J ml^{-1}), sieving, and water extraction.

2. Following the methods of Ellerbrock and Kaiser (2005), the solid residue of (1) was mixed with 50 ml 0.1 m $Na_4P_2O_7$ solution (pH 9–10) and shaken for 6 h with a rock and roll shaker. The sample was centrifuged and the supernatant decanted. The decanted supernatant was filtered through a 0.45 µm polyamide filter (Schleicher and Schuell, Dassel, Germany) and denoted as $OM(PY)_{total}$. The pH of the filtrate – $OM(PY)_{total}$ – was adjusted with 1 M HCl to pH 2 and cooled overnight in a refrigerator to precipitate organic matter. Then the mixture was centrifuged (35 min, 1400 × g) to separate the HCl soluble from the HCl insoluble (OM(PY): subfraction of $OM(PY)_{total}$) fraction. The reason for the separation of $Na_4P_2O_7$ soluble and HCl insoluble OM is to concentrate high molecular OM containing carboxylate functional groups in the OM(PY) fraction (Kaiser et al., 2011). $Na_4P_2O_7$ soluble

and insoluble in HCl (OM(PY)) as well as $Na_4P_2O_7$ soluble and soluble in HCl OM fractions were dialysed, and freeze dried.

3. The solid residue of (2) were washed with 0.1 m HCl and the $Na_4P_2O_7$ extraction was repeated as described for step (2) to remove the $Na_4P_2O_7$ soluble OM as complete as possible. The remaining extraction residue (ER) was washed with destilled water and freeze dried. The OM remaining in the ER (OM(ER)) can be prevented from extraction using H_2O and $Na_4P_2O_7$ (step 1 and 2) due to its chemical nature (less ionizable oxygen containing functional groups) and occlusion in aggregates not dispersed by ultrasonication (60 and 440 J ml^{-1}). The ER can contain organic particles < 63 µm that cannot be distinguished by eye from mineral particles. All extractions steps were done in 3 replicate samples.

2.4 Determination of the OC contents separated by the OM(PY) and OM(ER) fractions from the soil samples

The organic C content (Formacs TOC Analyser, SKALAR, Breda, Netherlands) in the OM(PY) fraction was determined from the C contents of the $OM(PY)_{total}$ fraction minus the C content of the OM fraction that is $Na_4P_2O_7$ and HCl soluble (Kaiser et al., 2011). This method was used because the precipitated $Na_4P_2O_7$ soluble and HCl insoluble OM(PY) can not be homogenized and directly measured. The freeze dried ER was homogenized by grinding in an agate mortar. The total C content in the ER was determined by elemental analysis (vario EL, ELEMENTAR, Hanau, Germany) and was assumed to be equivalent to the organic C (OC) content because the ER are free of carbonates. The data were normalized to 105 °C dry soil and given in g organic carbon (OC) per kg soil.

2.5 Determination of $\delta^{13}C$ and $\delta^{15}N$ of OM(PY) and OM(ER)

The isotope composition of the the OM(PY), and the OM(ER) fractions were analyzed at the Center for Agricultural Landscape Research Stable Isotope Laboratory.

A Thermo-Finnegan Flash HT elemental analyzer flash combusted the samples converting carbon and nitrogen to CO_2 and N_2 respectively, which were separated on a gas chromatograph column. The sample gas was flushed via a con-flow III to a Thermo-Scientific, Delta V advantage isotope ratio mass spectrometer. Calibration at this facility was to IAEA-CH-6 (sucrose) and IAEA-N-1 (ammonium sulphate). The isotopic values are expressed in delta notation (in ‰ units) , realteive to VPDB (Vienna Pee Dee Belemnite) for carbon and N_2 in air for nitrogen. Analysis of internal laboratory standards ensured that the estimates of the organic isotopic values were accurate to within 0.1‰.

2.6 Statistics

We used analysis of variance to test for differences in δ^{13}C and δ^{15}N signatures of OM(PY) and OM(ER) fractions between land use and soil type. We used partial least squares regression (PLS) to explain the variation in δ^{13}C and δ^{15}N of the different fractions attributed to the soil variables measured. PLS is commonly used to eliminate the problem of multicolinearity that occurs in regression when the number of independent variables is large compared to the number of the observations. Furthermore, PLS creates components that explain as much as possible the covariance in dependent and independent variables, unlike principle components analysis which reduces the dimensionality only in independent variables (Abdi, 2003; Geladi and Kowalski, 1986). While PLS is often used to create predictive models (Ekblad et al., 2005), we are primarily interested in using PLS to: (1) outline land use effects, and (2) identify mineral characteristics relevant for organo-mineral interactions across different soil types. Thus, in our analysis we grouped soil texture variables (contents of sand, silt, and clay particle-size fractions) to address differences between soil types. From PLS analysis we report percent of variance explained by the first three components, the weights of independent the variables on the third component, and regression coefficients of the PLS model to indicate magnitude and direction of each independent variable on the variability in the isotopic data.

3 Results

For OM(ER) fractions, a clear land use trend is apparent: OM(ER) of arable soils are primarily depleted in δ^{13}C and enriched in δ^{15}N while OM(ER) of forest soils are enriched in δ^{13}C and depleted in δ^{15}N (Fig. 1). Despite the trends in the data only the δ^{13}C between land use was significantly different ($P(F) < 0.03$) when the OM(ER) and OM(PY) fractions were grouped (Fig. 2); however, the differences between OM fractions were not significant when compiled by land use type (Fig. 3) or soil type (Fig. 4).

Given, that the difference in δ^{13}C of OM between arable and forest soils was significant, we grouped the data set by land use type for the Partial Least Square (PLS) analysis. The first three components of the PLS analysis explained 54–93% of the variance in the δ^{13}C data and 86–97% of the variance in δ^{15}N data for arable soils (Fig. 5). Contents of sand, silt and clay (i.e., texture) were strongly related to the first two components of the PLS analysis and thus, the texture explained much of the variation in the isotopic data of OM(PY) and OM(ER) for the arable soils; however, this was not the case for the forest soils except for the δ^{13}C of the OM(PY) fraction. Exchangable Ca (Ca_{ex}) heavily influenced the third component for all OM fractions of arable soils, which explained between 5% and 20% of the variation of δ^{13}C and δ^{15}N in the OM fractions from forests.

The impact of the measured variables on component three was analyzed through the weights calculated during PLS (Fig. 6a and b). The third component of the OM(ER) fraction for each of the two isotopes was impacted by the measured soil variables in a similar way: the weights of the variable on the component were either both positive or both negative for δ^{15}N and δ^{13}C. The opposite occurred in the OM(PY) fraction where the weights of the soil variables on the third component were consistently opposite from each other. When the third component of the δ^{15}N of the OM(PY) fraction was impacted negatively, the δ^{13}C of this fraction was impacted positively.

The regression coefficient of the PLS analysis reports the direction of the correlation to the isotopic data of the different OM fractions. For arable soils, the $\delta^{15}N_{ER}$ signatures

became more depleted with Ca_{ex} (Fig. 7a). This is in contrast to the $\delta^{15}N_{PY}$ which became more enriched with an increase in Ca_{ex}. The regression coefficient associated with soil texture, primarily contents of silt and sand, was less than 0.01 but given the high variation in texture among soils, the impact on the ensuing isotopic composition could be large. For $\delta^{15}N_{ER}$ of, an increase in silt and sand contents resulted in depleted values whereas for $\delta^{13}C_{ER}$, an increase in the silt content led to depleted values and an increase in the sand content to enriched values.

For forest soils, $\delta^{15}N_{ER}$ and $\delta^{15}N_{PY}$ signatures became more enriched with an increase in the ratio of SOC and specific surface area (SOC/SSA) (Fig. 7b). An increase in clay, silt and sand contents resulted in enriched $\delta^{15}N_{ER}$ and $\delta^{13}C_{PY}$ signals whereas decreased silt and sand contents resulted in depleted $\delta^{15}N_{PY}$ and $\delta^{13}C_{ER}$ signals.

4 Discussion

In this research, we set out to explore whether or not the isotopic signal of OM fractions sequentially separated from a range of soil types under arable and forest land use would yield additional information about microbial transformations and insights into the type of interaction between OM and soil minerals. The investigated OM(PY) and OM(ER) fractions are both hypothesized to contain stabilized OM, but given their differences in extractability we expected differences in the interaction with the various compounds present in soil.

The impact of soil texture (i.e., clay, silt, and sand content) was overwhelming in explaining the isotopic variation in OM(PY) and OM(ER) of arable soils in our study. In contrast, texture explained little of the isotopic variation in OM fractions of the forest soils except for $\delta^{13}C_{PY}$. Relations between soil texture and stabilized OM are well established (Chenu and Plante, 2006; Six et al., 2002) and the driving question behind this research is to reach beyond this empirical relationship and determine whether or not we can identify how OM is bound to soil mineral particles. This explains why we

used PLS analysis. The variation in our data that can be attributed to soil particle size distribution is accounted for by the first two PLS components. Thus, the third component is orthogonal to the first two components and allows us to investigate further the relationship between isotopic patterns and proxies for soil mineral characteristics. We analyzed five arable and five forest topsoil samples, but the different soil types could obscure significant land use patterns. Thus, PLS allowed us to analyze OM that is most susceptible to land use impacts by factoring out the influence of soil type in our analysis.

4.1 Isotopic patterns in arable soils

We found that variation in $\delta^{15}N_{ER}$ and $\delta^{15}N_{PY}$ of the arable soils was related to Ca_{ex} content. Interestingly, the Ca_{ex} level correlated differently to each fraction in the regression model: a negative correlation with $\delta^{15}N_{ER}$ and a positive correlation with $\delta^{15}N_{PY}$, an indication of different nitrogen processing or sources. From a soil biological perspective, the relationship between Ca and N is largely thought of in terms of the specific activity of microbial cells: the more Ca (base cations) the more microbial activity due to higher pH values (Groffman et al., 2006). Thus, the pattern of $\delta^{15}N_{PY}$ enrichment with an increase of Ca_{ex} is consistent with the hypothesis of enhanced microbial transformation (Bostrom et al., 2007; Sollins et al., 2009). Moreover, Ca plays an important role in cation mediated interactions between organic molecules and mineral surfaces (Clough and Skjemstad, 2000; Wuddivira and Camps-Roach, 2007) or between different organic molecules, a process decribed as “crosslinking” (e.g., Subramaniam et al., 2004). According to Oades (1988), the effect of adding Ca to soil is a transient acceleration of OM decomposition and a long term effect of stabilization. Therefore, we hypothesize an increased stabilization of microbial processed OM(PY) via OM(PY)-Ca-mineral, OM(PY)-Ca (i.e., chelates) and/or OM(PY)-Ca-OM(PY) (i.e., crosslinking) (Subramaniam et al., 2004; Yang et al., 2001) interactions with increasing Ca_{ex} contents.

The pattern of a depleted $\delta^{15}N_{ER}$ signal with higher soil Ca content has not been observed before and processes that lead to this pattern are unclear. We hypothesize that the isotopic composition of OM(ER) is influenced by $\delta^{15}N$ depleted OM of previous forest ecosystems still present in soils due to occlusion in soil micro-structures. We base this hypothesis on the methodology of OM separation we used. We sequentially separated at first organic particles (> 63 µm) and water-extractable OM in combination with a stepwise dispersion of macro- and micro-aggregates (using ultrasonic energy: 60 and 400 J ml^{-1}) followed by an extraction of OM(PY) from soil samples. The extraction residue after this treatments can contain physically highly stable, clay and silt sized micro-structures only dispersible by energy amounts > 440 J ml^{-1} (Chenu and Plante, 2006; Zhu et al., 2009; Moni et al., 2010) preserving OM occluded in such structures from separation. The $\delta^{15}N_{ER}$ patterns show little sign of degradation or microbial transformation for OM(ER) indicating that nitrogenous compounds in this fraction are highly protected from microbial processing or the energy cost to release the N compounds is too high. Despite the uncertainty in mechanisms responsible for the $\delta^{15}N_{ER}$ signatures, we can infer that the methodology is successful at separating fractions of OM that contain organic carbon from different sources.

4.2 Isotopic patterns in forest soils

In forest soils, the third component for all OM fractions, which explained up to 55% and 80% of the variation in $\delta^{13}C$ and $\delta^{15}N$, respectively, was largely driven by the SOC content and the SOC/SSA ratio. Reports in the literature have suggested that an increase in the SOC/SSA ratio indicates an increase in the number of OM layers covering mineral surfaces (Keil et al., 1994; Koegel-Knaber et al., 2008). The SOC/SSA ratios in soils of this study ranged from 0.6 to 59.62 g m^{-2}, with all exceeding 1 mg OC per m^{-2} SSA, the theoretical lower threshold for multi-layering of OM on mineral surfaces. The isotopic signatures of $\delta^{13}C_{ER}$ and $\delta^{13}C_{PY}$ were influenced by SOC and SOC/SSA ratios in contrasting directions. $\delta^{13}C_{PY}$ signature tended to become enriched with an

increase in SOC levels while $\delta^{13}C_{ER}$ incorporated less of the heavy isotope, reflected by a depleted isotopic signature. The pattern of enrichment in $\delta^{13}C_{PY}$ with SOC/SSA levels is an indication of microbial processing of OM. This pattern is shared with both $\delta^{15}N_{PY}$ and $\delta^{15}N_{ER}$ thus, reinforcing the interpretation of microbially processed organic matter sequentially layered on soil mineral surfaces (Kleber et al., 2007; Huygens et al., 2008; Sollins et al., 2009). However, this did not occur with OM(ER) where $\delta^{13}C$ values decreased with increasing SOC levels. It is likely, that the OM in the ER fraction has undergone a different pathway to stabilization that does not involve microbial processing or perhaps it reflects a high level of protection within soil micro-structures, similar to the OM(ER) of the arable soil. Bachmann et al. (2008) posit that "there are several lines of evidence that organic matter covers minerals in a patchy manner and that even at the nanoscale organic matter and minerals aggregate". This is confirmed by findings of Chenu and Plante (2006) who found that many of so called "clay particles" were nanometer to micrometer-sized micro-aggregates in which OM was encrusted by minerals. The authors concluded that these very small micro-aggregates protect OM from decomposition "by adsorption and by entrapment of organic matter".

4.2.1 Molecular model application

We can infer relationships between the isotopic signatures of OM fractions and soil characteristics. Applying the isotopic patterns within the context of the conceptual zonal model proposed by Kleber et al. (2007) an overall picture of OM dynamics and stabilization in soils under arable and forest land use may be achieved. The model of Kleber et al. (2007) describes OM interactions with minerals within three zones: a contact zone, hydrophobic zone, and a kinetic zone. Within each zone the force of attraction is different: the contact zone represents the strongest attraction while in the kinetic zone organic matter is loosely bound. Within each zone the authors describe potential mechanisms that may lead to the binding of OM. In the arable soils, Ca_{ex} played a large role in driving the $\delta^{15}N$ patterns of OM(PY). The $\delta^{15}N_{PY}$ of ^{15}N

enrichment with increasing Ca_{ex} can be a result of separating OM(PY) from the contact zone where OM can bound to mineral surfaces via cation bridging by Ca_{ex}. In contrast, the $\delta^{15}N_{ER}$ became depleted with increasing Ca_{ex} which suggests that the OM in the ER fraction was not from the contact zone. The OM in the ER fraction may be located within micro-aggregates rendering the N in this fraction inaccessible to microorganisms or, potentially, the N in this fraction could be proteinaceous material covering the mineral surface in the contact zone.

The absence of a strong correlation of component 3 and the $\delta^{13}C_{PY}$ or $\delta^{13}C_{ER}$ patterns in the arable soils, indicates a small amount of carbon in these fractions is not interacting with mineral surfaces or is not occluded in microstructures (represented by PLS component 1) and is, therefore, readily available for exchange. The carbon could derive from organic particles $< 63\,\mu m$ not separated during soil fractionation. Alternatively, the carbon could be derived from OM present in the the kinetic zone. Evidence for carbon exchanging in the kinetic zone can also be found in ^{14}C studies where labeled C is found in organo-mineral complexes, which are long thought to be stable because of long residence times (Swanston et al., 2005; Bruun et al., 2008).

Interestingly, in the forest soil, both the $\delta^{13}C_{PY}$ and $\delta^{15}N_{PY}$ values become enriched with the increase in the ratio of SOC/SSA. A high SOC/SSA ratio ($> 1\,mg\,m^{-2}$) implies multiple layers of OM attached to mineral surfaces, and as indicated by isotopic signature of the OM(PY), the OM in these layers is highly processed by microorganisms. The pattern in the enriched isotopic signals suggests that OM in these layers exhibit slow exchange kinetics. A potential mechanism can be the crosslinking of OM in such layers via polyvalent cations (Subramaniam et al., 2004; Yang et al., 2001).

5 Conclusions

The isotopic signatures of OM fractions from arable soils are related to contents of the clay and silt size particles and Ca_{ex}, while for forest soils only a relation to SOC/SSA was identified. Thus, we infer different binding mechanisms predominate in each land

use type. For arable soils, the formation of OM(PY)-Ca-mineral associations is OM stabilization mechanism while the OM(PY) of forest soils is separated from layers of slower exchange not directly attached to mineral surfaces. This means there is a potential to build multiple OM layers on mineral particles in the arable soil and thus the potential for carbon accumulation. The $\delta^{13}C_{PY}$ and $\delta^{13}C_{ER}$ values of the arable soils were found to be generally depleted (except HC, $\delta^{13}C_{ER}$) as compared to respective forest soils. A greater number of microorganisms or an increased level of microbial metabolic activity in the forest soils (Kaiser et al., 2010) could explain this pattern. Although, the carbon fixed by trees and deposited in the soil was likely carboxylated at an earlier date than the arable vegetation. This would result in forest OM having a more enriched isotopic signal due to the Suess effect (the depletion in atmospheric CO_2 over time as a function of an increase in fossil fuel combustion). Future studies, with higher replications among soil types and assessing sites where land use change occurred at different time points will be necessary to elucidate these patterns.

Acknowledgements. The study was financially supported by the Deutsche Forschungsgemeinschaft, Bonn (DFG) under grant KA 2652 (1-1 and 1-2).

References

Bachmann, J., Guggenberger, G., Baumgartl, T., Ellerbrock, R. H., Urbanek, E., Goebel, M.-O., Kaiser, K., Horn, R., and Fischer, W. R.: Physical carbon-sequestration mechanisms under special consideration of soil wettability, J. Plant Nutr. Soil Sc., 171, 14–26, doi:10.1002/jpln.200700054, 2008.

Baldock, J. A. and Nelson, P. N.: Soil organic matter, in: Handbook of Soil Sciences, edited by: Summer, M. E., CRC Press, Boca Raton, FL, USA, 1325–1382, 2000.

Boström, B., Comstedt, D., and Ekblad, A.: Isotope fractionation and ^{13}C enrichment in soil profiles during the decomposition of soil organic matter, Oecologia, 153, 89–98, doi:10.1007/s00442-007-0700-8, 2007.

Chenu, C. and Plante, A. F.: Clay-sized organo-mineral complexes in a cultivation chronose-

quence: revisiting the concept of the 'primary organo-mineral complex', Eur. J. Soil Sci., 57, 596–607, doi:10.1111/j.1365-2389.2006.00834.x, 2006.
Clay, D. E., Clapp, C. E., Reese, C., Liu, Z., Carlson, C. G., Woodard, H., and Bly, A.: Carbon-13 Fractionation of Relic Soil Organic Carbon during Mineralization Effects Calculated Half-Lives, Soil Sci. Soc. Am. J., 71, 1003–1009, doi:10.2136/sssaj2006.0193, 2007.
Clough, A. and Skjemstad, J. O.: Physical and chemical protection of soil organic carbon in three agricultural soils with different contents of calcium carbonate, 5, CSIRO Publishing, Collingwood, Australia, 2000.
Ekblad, A., Bostrom, B., Holm, A., and Comstedt, D.: Forest soil respiration rate and delta C-13 is regulated by recent above ground weather conditions, Oecologia, 143, 136–142, 2005.
Ellerbrock, R. H. and Kaiser, M.: Stability and composition of different soluble soil organic matter fractions – evidence from δ^{13}C and FTIR signatures, Geoderma, 128, 28–37, 2005.
Geladi, P. and Kowalski, B. R.: Partial least-squares regression: a tutorial, Anal. Chim. Acta, 185, 1–17, 1986.
Groffman, P., Fisk, M., Driscoll, C., Likens, G., Fahey, T., Eagar, C., and Pardo, L.: Calcium Additions and Microbial Nitrogen Cycle Processes in a Northern Hardwood Forest, Ecosystems, 9, 1289–1305, doi:10.1007/s10021-006-0177-z, 2006.
Haile-Mariam, S., Collins, H. P., Wright, S., and Paul, E. A.: Fractionation and Long-Term Laboratory Incubation to Measure Soil Organic Matter Dynamics, Soil Sci. Soc. Am. J., 72, 370–378, doi:10.2136/sssaj2007.0126, 2008.
Kaiser, K. and Guggenberger, G.: Mineral surfaces and soil organic matter, Eur. J. Soil Sci., 54, 219–236, doi:10.1046/j.1365-2389.2003.00544.x, 2003.
Kaiser, M., Ellerbrock, R. H., and Sommer, M.: Separation of Coarse Organic Particles from Bulk Surface Soil Samples by Electrostatic Attraction, Soil Sci. Soc. Am. J., 73, 2118–2130, doi:10.2136/sssaj2009.0046, 2009.
Kaiser, M., Walter, K., Ellerbrock, R. H., and Sommer, M.: Effects of land use and mineral characteristics on the organic carbon content, and the amount and composition of Na-pyrophosphate-soluble organic matter, in subsurface soils, Eur. J. Soil Sci., doi:10.1111/j.1365-2389.2010.01340.x, 2011.
Kleber, M. and Johnson, M. G.: Advances in Understanding the Molecular Structure of Soil Organic Matter: Implications for Interactions in the Environment, in: Advances in Agronomy, edited by: Donald, L. S., Academic Press, 77–142, 2010.
Kleber, M., Mikutta, R., Torn, M. S., and Jahn, R.: Poorly crystalline mineral phases protect

organic matter in acid subsoil horizons, Eur. J. Soil Sci., 56, 717–725, doi:10.1111/j.1365-2389.2005.00706.x, 2005.
Kleber, M., Sollins, P., and Sutton, R.: A conceptual model of organo-mineral interactions in soils: self-assembly of organic molecular fragments into zonal structures on mineral surfaces, Biogeochemistry, 85, 9–24, doi:10.1007/s10533-007-9103-5, 2007.
Kögel-Knabner, I., Guggenberger, G., Kleber, M., Kandeler, E., Kalbitz, K., Scheu, S., Eusterhues, K., and Leinweber, P.: Organo-mineral associations in temperate soils: Integrating biology, mineralogy, and organic matter chemistry, J. Plant Nutr. Soil Sc., 171, 61–82, doi:10.1002/jpln.200700048, 2008.
Liao, J. D., Boutton, T. W., and Jastrow, J. D.: Organic matter turnover in soil physical fractions following woody plant invasion of grassland: Evidence from natural ^{13}C and ^{15}N, Soil Biol. Biochem., 38, 3197–3210, 2006.
Lützow, M. V., Kögel-Knabner, I., Ekschmitt, K., Matzner, E., Guggenberger, G., Marschner, B., and Flessa, H.: Stabilization of organic matter in temperate soils: mechanisms and their relevance under different soil conditions – a review, Eur. J. Soil Sci., 57, 426–445, doi:10.1111/j.1365-2389.2006.00809.x, 2006.
Marin-Spiotta, E., Silver, W. L., Swanston, C. W., and Ostertag, R.: Soil organic matter dynamics during 80 years of reforestation of tropical pastures, Glob. Change Biol., 15, 1584–1597, doi:10.1111/j.1365-2486.2008.01805.x, 2009.
Masiello, C. A., Chadwick, O. A., Southon, J., Torn, M. S., and Harden, J. W.: Weathering controls on mechanisms of carbon storage in grassland soils, Glob. Biogeochem. Cycles, 18, GB4023, doi:10.1029/2004gb002219, 2004.
Mikutta, R., Kleber, M., Torn, M., and Jahn, R.: Stabilization of Soil Organic Matter: Association with Minerals or Chemical Recalcitrance?, Biogeochemistry, 77, 25–56, doi:10.1007/s10533-005-0712-6, 2006.
Moni, C., Rumpel, C., Virto, I., Chabbi, A., and Chenu, C.: Relative importance of sorption versus aggregation for organic matter storage in subsoil horizons of two contrasting soils, Eur. J. Soil Sci., 61, 958–969, doi:10.1111/j.1365-2389.2010.01307.x, 2010.
Oades, J.: The retention of organic matter in soils, Biogeochemistry, 5, 35–70, doi:10.1007/bf02180317, 1988.
Six, J., Conant, R. T., Paul, E. A., and Paustian, K.: Stabilization mechanisms of soil organic matter: Implications for C-saturation of soils, Plant Soil, 241, 155–176, doi:10.1023/a:1016125726789, 2002.

Sollins, P., Kramer, M., Swanston, C., Lajtha, K., Filley, T., Aufdenkampe, A., Wagai, R., and Bowden, R.: Sequential density fractionation across soils of contrasting mineralogy: evidence for both microbial- and mineral-controlled soil organic matter stabilization, Biogeochemistry, 96, 209–231, doi:10.1007/s10533-009-9359-z, 2009.

Solomon, D., Fritzsche, F., Lehmann, J., Tekalign, M., and Zech, W.: Soil Organic Matter Dynamics in the Subhumid Agroecosystems of the Ethiopian Highlands, Soil Sci. Soc. Am. J., 66, 969–978, doi:10.2136/sssaj2002.0969, 2002.

Subramaniam, K., Stepp, C., Pignatello, J. J., Smets, B., and Grasso, D.: Enhancement of polynuclear aromatic hydrocarbon desorption by complexing agents in weathered soil, Environ. Eng. Sci., 21, 515–523, 2001.

Trumbore, S.: Radiocarbon and Soil Carbon Dynamics, Annu. Rev. Earth Planet. Sci., 37, 47–66, doi:10.1146/annurev.earth.36.031207.124300, 2009.

von Lützow, M., Kögel-Knabner, I., Ekschmitt, Matzner, E., Guggenberger, G., Marschner, B., and Flessa, H.: Stabilization of organic matter in temperate soils: mechanisms and their relevance under different soil conditions – a review, Eur. J. Soil Sci., 57, 426–455, 2006.

von Lützow, M., Kögel-Knabner, I., Ekschmitt, K., Flessa, H., Guggenberger, G., Matzner, E., and Marschner, B.: SOM fractionation methods: Relevance to functional pools and to stabilization mechanisms, Soil Biol. Biochem., 39, 2183–2207, 2007.

Wattel-Koekkoek, E. J. W., Buurman, P., Van Der Plicht, J., Wattel, E., and Van Breemen, N.: Mean residence time of soil organic matter associated with kaolinite and smectite, Eur. J. Soil Sci., 54, 269–278, doi:10.1046/j.1365-2389.2003.00512.x, 2003.

Wuddivira, M. N. and Camps-Roach, G.: Effects of organic matter and calcium on soil structural stability, Eur. J. Soil Sci., 58, 722–727, doi:10.1111/j.1365-2389.2006.00861.x, 2007.

Yang, Y., Ratté, D., Smets, B. F., Pignatello, J. J., and Grasso, D.: Mobilization of soil organic matter by complexing agents and implications for polycyclic aromatic hydrocarbon desorption, Chemosphere, 43, 1013–1021, 2001.

Zhu, Z. L., Minasny, B., and Field, D. J.: Measurement of aggregate bond energy using ultrasonic dispersion, Eur. J. Soil Sci., 60, 695–705, doi:10.1111/j.1365-2389.2009.01146.x, 2009.

Table 1. Soil classification, coordinates, altitude, and climatic parameters for the different study sites.

Site name	Soil classification	Geographical position			Climatic parameters	
		Longitude (°E)	Latidue (°N)	Altitude (m a.s.l.)	Precipitation (mm yr^{-1})	Temperature (°C)
Rowa	AL: Albic Luvisol	13°16′20″	53°29′47″	90	536[c]	7.9[c]
Elmenhorst	HSt: Haplic Stagnosol	13°02′19″	54°12′14″	23	566[d]	8.0[d]
Simmringen	HL: Haplic Luvisol	09°52′57″	49°34′47″	338	577[e]	9.4[e]
Nellingen	HC: Haplic Cambisol	09°46′18″	48°33′16″	710	1069[f]	6.8[f]
Herrenberg	VC: Vertic Cambisol	08°56′13″	48°33′59″[a]	420	795[g]	8.3[g]
Herrenberg	VC: Vertic Cambisol	08°56′31″	48°33′12″[b]	420	795[h]	8.3[h]

Coordinates and altitude were taken from topographical maps with a scale of 1:25 000; [a] coordinates for the agricultural soil; [b] coordinates for the forest soil. Soil classification was done according to WRB (2006). Climatic parameters are mean values recorded from the following climatic stations and years: [c] Neubrandenburg: 1961–1990; [d] Greifswald: 1961–1990; [e] Würzburg: 1971–2000; [f]Geislingen-Stötten: 1961–1990; [g] Rottenburg: 1961–1990.

Table 2. Land use, and depth, as well as mean values of pH, and contents of sand, silt, clay, soil organic carbon (SOC; determined after the separation of organic particles by electrostatic attraction), oxalate soluble Fe, Al (Fe_{ox}, Al_{ox}) as well as exchangeable Ca (Ca_{ex}) of the arable (Ap) and forest (Ah) topsoil samples from the Albic Luvisol (AL), Haplic Stagnosol (HSt), Haplic Luvisol (HL), Haplic Cambisol (HC), and Vertic Cambisol (VC) sites.

Soil	Land use	Horizon	Horizon Depth (cm)	pH[a] $CaCl_2$	Texture Sand[b] $g\,kg^{-1}$	Silt[c] $g\,kg^{-1}$	Clay[d] $g\,kg^{-1}$	SOC $g\,kg^{-1}$	SSA $m^2\,g^{-1}$	Fe_{ox} $mg\,kg^{-1}$	Al_{ox} $mg\,kg^{-1}$	Ca^{e}_{ex} $cmol_c\,kg^{-1}$
AL	Arable	Ap	0–25	6.7	592	348	69	7.8 (± 0.18)	2.92	1372 (± 2)	500 (± 2)	3.4
	Forest	Ah	1/2–5/10[f]	3.4	616	341	63	47.1 (± 0.97)	0.79	1886 (± 10)	782 (± 16)	0.5
HST	Arable	Ap	0–30	7.4	610	290	113	10.7 (± 0.02)	4.09	1591 (± 33)	451 (± 15)	7.6
	Forest	Ah	2/3–10	3.6	650	279	90	31.0 (± 0.01)	1.41	2256 (± 38)	1115 (± 7)	1.3
HL	Arable	Ap	0–20	7.5	45	799	174	9.3 (± 0.05)	10.97	3252 (± 174)	588 (± 21)	11.2
	Forest	Ah	1/2–15/20	3.7	46	833	143	35.6 (± 0.12)	5.87	4048 (± 120)	1121 (± 5)	4.0
HC	Arable	Ap	0–8/12	7	45	619	380	26.8 (± 0.34)	17.52	5086 (± 73)	2139 (± 8)	25.1
	Forest	Ah	0.5/1–7/10	4.3	24	624	399	37.1 (± 0.05)	21.40	4052 (± 22)	2906 (± 40)	8.9
VC	Arable	Ap	0–5/8	7.1	108	384	561	22.6 (± 0.57)	34.41	2848 (± 105)	1382 (± 9)	20.8
	Forest	Ah	1/3–25/30	4.5	80	599	352	14.3 (± 0.17)	23.68	4006 (± 120)	1343 (± 24)	4.2

Values in parenthesis are single standard errors ($n = 2$). [a]SD ($n = 2$) is less than or equal to ± 0.14. [b]SD ($n = 2$) is less than or equal to ± 11. [c]SD ($n = 2$) is less than or equal to ± 11. [d]SD ($n = 2$) is less than or equal to ± 3. [e]SD ($n = 2$) is less than or equal to ± 0.08. [f]means here, for example, upper boundary of the horizons between 1 and 2 cm depth and lower boundary of the horizons between 5 and 10 cm depth

Table 3. Contents of organic carbon as well as $\delta^{13}C$ and $\delta^{15}N$ signatures of organic matter sequentially separated by Na-pyrophosphate solution (OC_{PY}, $\delta^{13}C_{PY}$, $\delta^{15}N_{PY}$) and remaining in the extraction residue (OC_{ER}, $\delta^{13}C_{ER}$, $\delta^{15}N_{ER}$), as well as the relative proportion of OC_{PY} and OC_{ER} contents in soil organic carbon (SOC) contents for the arable (Ap) and forest (Ah) topsoil samples from the Albic Luvisol (AL), Haplic Stagnosol (HSt), Haplic Luvisol (HL), Haplic Cambisol (HC), and Vertic Cambisol (VC) sites.

Soil	Horizon	OC_{PY} $(g\,kg^{-1})$	OC_{PY}/SOC (%)	$\delta^{13}C_{PY}$	$\delta^{15}N_{PY}$	OC_{ER} $(g\,kg^{-1})$	OC_{ER}/SOC (%)	$\delta^{13}C_{ER}$	$\delta^{15}N_{ER}$
AL	Ap	0.58 (± 0.04)	7.4	−25.50	3.91	4.4 (± 0.10)	56.8	−26.02	4.54
	Ah	9.14 (± 0.55)	19.4	−25.46	6.64	16.8 (± 1.37)	35.6	−25.11	6.71
HST	Ap	1.13 (± 0.02)	10.6	−25.77	5.08	5.5 (± 0.12)	51.4	−26.36	5.85
	Ah	4.14 (± 0.22)	13.3	−25.68	−1.09	13.3 (± 0.23)	42.9	−25.22	2.94
HL	Ap	0.57 (± 0.02)	6.2	−25.80	3.17	5.4 (± 0.13)	58.1	−25.50	4.44
	Ah	10.95 (± 1.05)	30.8	−25.18	−0.08	16.6 (± 0.47)	46.8	−24.89	2.61
HC	Ap	4.47 (± 0.18)	16.7	−25.45	5.54	17.9 (± 0.32)	66.9	−24.93	−0.93
	Ah	5.2 (± 0.42)	14	−23.36	3.23	19.0 (± 0.32)	51.1	−25.37	6.45
VC	Ap	2.01 (± 0.1)	8.9	−25.42	5.56	16.3 (± 0.29)	72.3	−25.14	1.24
	Ah	1.29 (± 0.04)	9	−25.03	3.80	7.9 (± 0.07)	55.1	−24.41	0.38

Values in parenthesis are standard errors ($n = 3$).

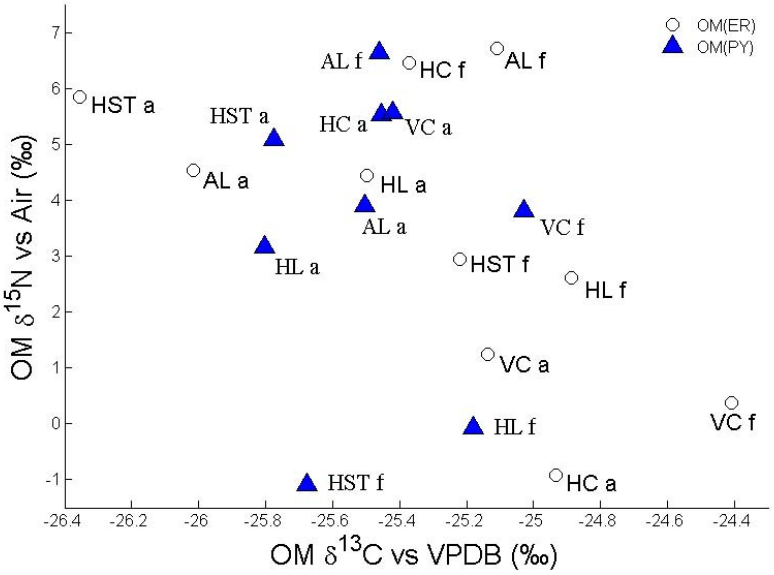

Fig. 1. Isotopic composition (δ^{15}N, δ^{13}C) of the OM(PY) and OM(ER) fractions sequentialy separated from the arable and forest soils. Soil types (see Table 1 for abbreviations) and land use types abbreviations (a = arable, f = forest) appear next to each data point.

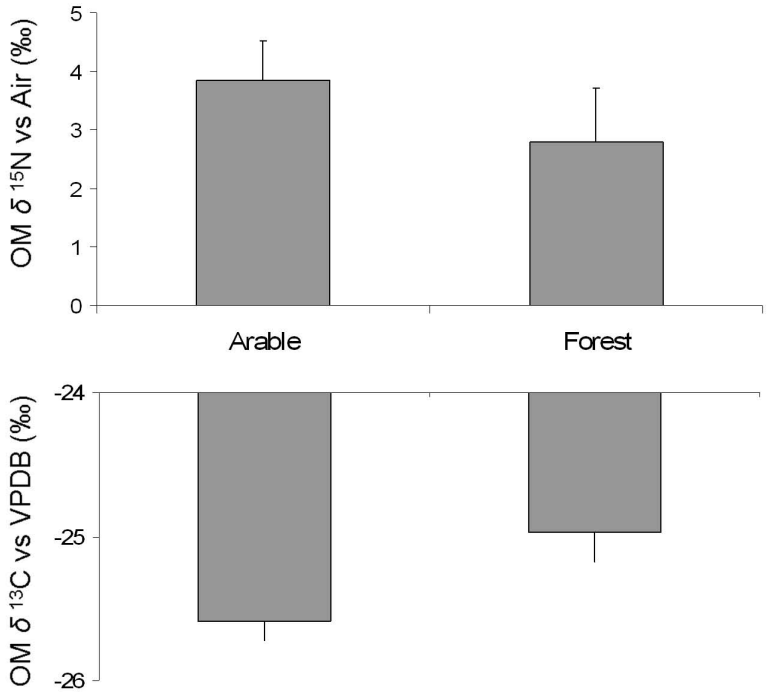

Fig. 2. Comparison of the isotopic composition of compiled OM fractions in arable and forest land use types. The difference between land use type is significant ($p < 0.03$). The y axis is divided by stable isotope, ^{15}N is shown on top, and ^{13}C is shown below. Note: To highlight the differences between land use types, different scales are used for each isotope. Error bars are standard error of the mean.

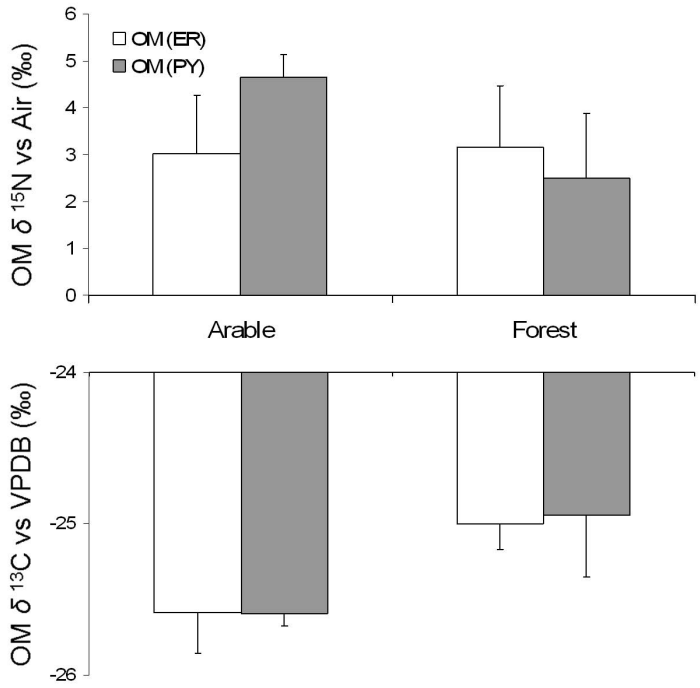

Fig. 3. Comparison of the isotopic composition of OM(ER) and OM(PY) in arable and forest land use types. The differences are not significant when the data are grouped by OM fractions and land use type. The y axis is divided by stable isotope, ^{15}N is shown on top, and ^{13}C is shown below. Note: To highlight the differences between land use types, different scales are used for each isotope. Error bars are standard error of the mean.

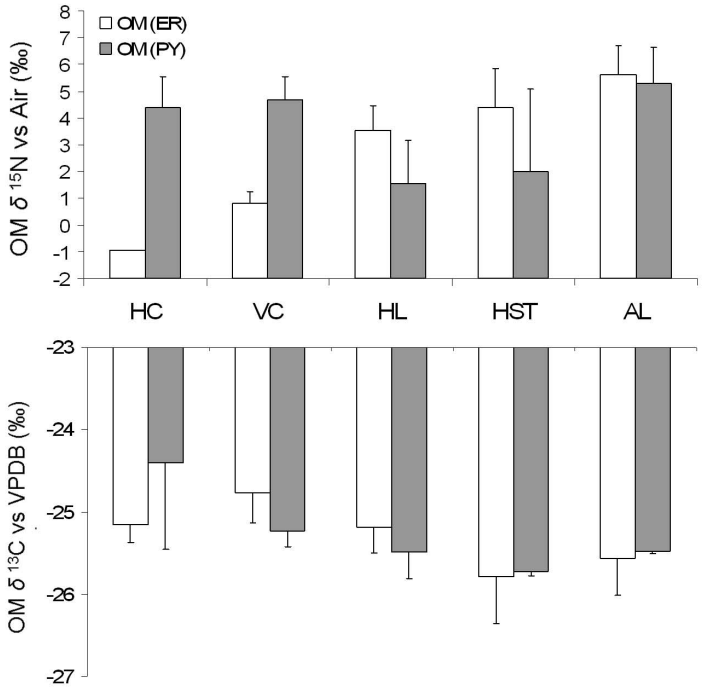

Fig. 4. Comparison of the isotopic composition of OM(ER) and OM(PY) across different soil types. The differences between OM fractions were not significant when grouped by soil type (i.e. irrespective of land use type) The y axis is divided by stable isotope, ^{15}N is shown on top, and ^{13}C is shown below. Note: To highlight the differences between soil use types, different scales are used for each isotope. Error bars are standard error of the mean.

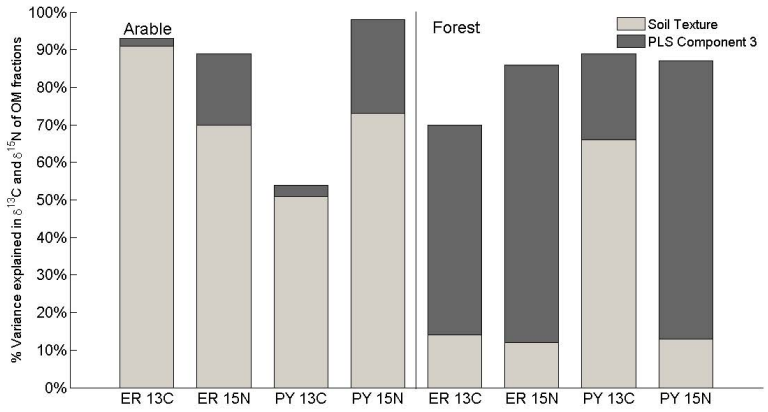

Fig. 5. Variance in the isotopic data (y-axis) in OM fractions (x-axis) explained by the first three components of the PLS analysis. The first two components were highly correlated with soil texture (distribution of sand, silt, clay) and were combined. PLS component 3 is orthogonal to the first two components, therefore, the variation explained and the subsequent models are related to soil mineral proxies.

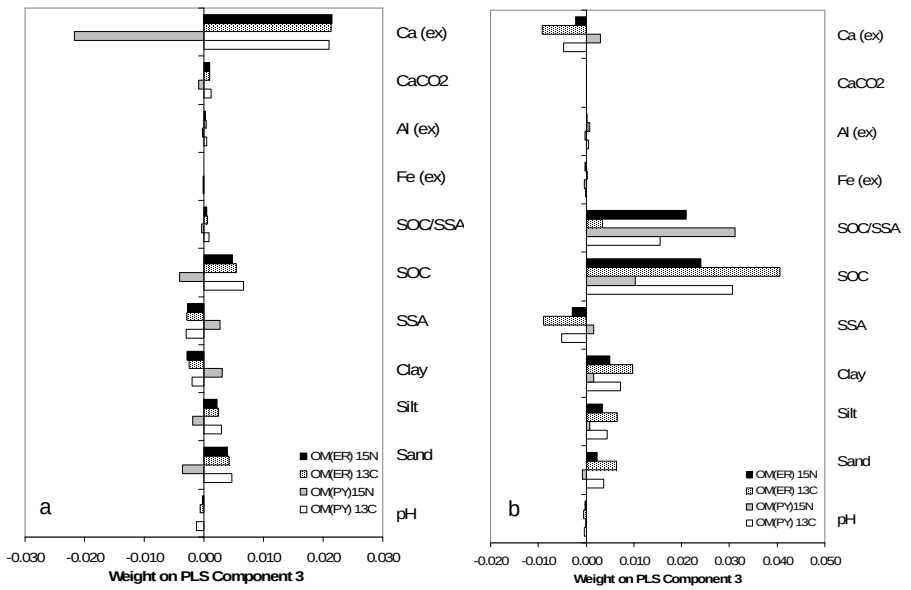

Fig. 6. PLS weights of soil parameter of each soil parameter of arable soil **(a)** and forest soil **(b)** on the isotopic signature of different OM fractions represented in component 3.

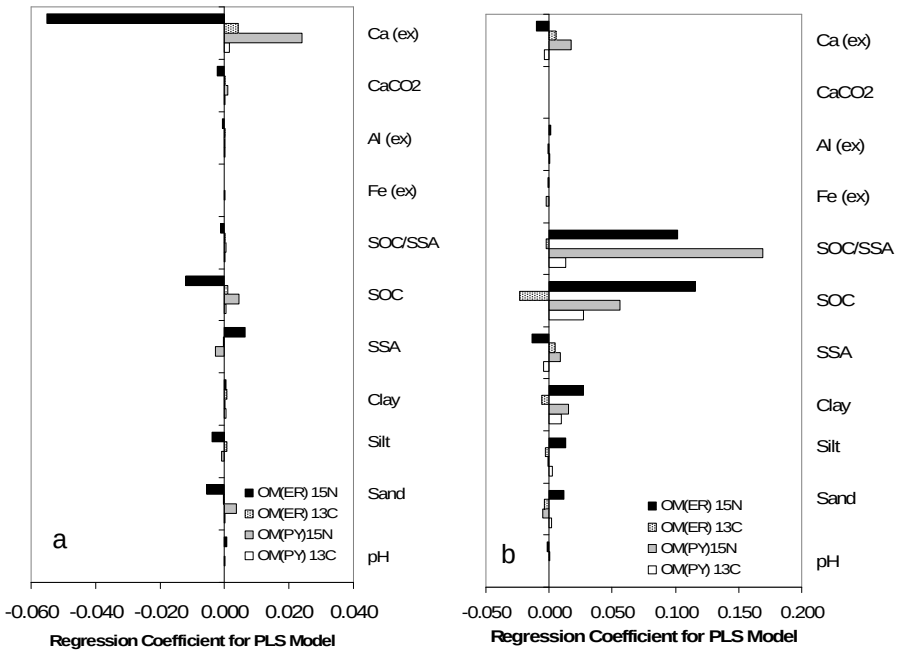

Fig. 7. PLS regression coefficients of each soil parameter of arable soil **(a)** and forest soil **(b)** on the isotopic signature of different OM fractions represented in component 3.